Proc. of the 7th Communication Theory Mini–Conference (CTMC at Globecom'98), pp.201-206, Nov. 1998, Sydney, Australia

ANALYSIS OF A FRAME- AND FREQUENCY SYNCHRONIZER FOR (BURSTY) OFDM

Stefan H. Müller–Weinfurtner, Jürgen F. Rößler, and Johannes B. Huber

Laboratorium für Nachrichtentechnik, Universität Erlangen–Nürnberg
Cauerstraße 7, D–91058 Erlangen, Germany
e-mail: *smueller@nt.e-technik.uni-erlangen.de*, WWW: *http://www-nt.e-technik.uni-erlangen.de/~dcg*

Abstract — Analytical results for a frame- and carrier frequency synchronization scheme with repetition preamble [2] are derived. When such a preamble is composed of random Orthogonal Frequency–Division Multiplexing (OFDM) symbols with cyclic prefix, a surprising statistical effect occurs in non–dispersive channels; the lock–in probability of the frame synchronizer is non–uniformly distributed inside the valid synchronization range. This effect is illuminated with a theory which perfectly corresponds to simulation results. Furthermore, we provide an expression for the variance of the normalized frequency estimate in the presence of frame synchronization errors. This result can be used to design the required preamble length to achieve a prescribed burst frequency accuracy.

1. Introduction

OFDM offers advantages in transmission over (severe) multipath channels [11]. Hence, there is an increased interest in applying OFDM for high–rate mobile data transmission [1]. We mention wireless Asynchronous Transfer Mode (ATM) as one potential field of interest [9], where packet–oriented transmission requires burst synchronization schemes which allow reliable single–shot frame- and carrier frequency synchronization with as minimum as possible preamble overhead.

The general principle of a cyclic training signal for frame synchronization and carrier frequency offset estimation in transmission scenarios over unknown dispersive channels was originally suggested for single–carrier transmission in [2]. In [2, 4] the preamble is composed of repeated single–carrier data. We want to focus on the repetition of entire OFDM symbols introduced in [6] and further investigated in [12, 13]. In our investigation, the repeated OFDM symbol carries data. Hence, this data is reliably received with a time–diversity factor of two and the preamble itself is — apart from the periodicity — random and not purely training overhead.

The paper is organized as follows: After the description of the transmission model in Section 2, the burst synchronization criteria are introduced and their respective performance is presented in Section 3 by means of simulation as well as analytical results. Section 4 is dedicated to conclusions.

This work was supported by Ericsson Eurolab Deutschland GmbH in Nürnberg and is funded in parts by the national research initiative ATMmobil of the German Ministery for Research and Education (BMBF).

J. Rößler is now with Siemens Automobiltechnik AT PT SI TSA 172, D–93055 Regensburg, Germany.

2. Transmission Model

We consider an OFDM burst transmission system. The burst consists of several regular OFDM symbols, each generated with a D–dimensional inverse discrete Fourier transform (IDFT). The modulation interval (transmit sample spacing) for the system is denoted by T, so that the Nyquist bandwidth of the entire multiplex signal is $1/T$. Thus, the regular subcarrier spacing is $\Delta f_{\mathrm{sub}} = \frac{1}{DT}$. The synchronization preamble precedes the burst and consists of two identical D_{s}–carrier OFDM symbols — the first of which starting at discrete–time position $k = 0$. We mention that we gain an additional degree of freedom by not necessarily choosing D_{s} equal to D, like it is the case in [6, 12]. This implies that the preamble OFDM symbol can be chosen smaller ($D_{\mathrm{s}} < D$) to reduce overhead. The first of these two identical OFDM symbols is equipped with a guard interval of D_{g} samples located in time positions $k = -D_{\mathrm{g}}$ through -1. The guard interval is a cyclic extension of some discrete–time samples [11]. The periodicity in the preamble is symbolized by the similarity of triangle shapes in Fig. 1a. Note that because of symbol repetition the tail of the first symbol simultaneously represents the guard interval for the second, so that the overall preamble length is only $2D_{\mathrm{s}} + D_{\mathrm{g}}$. Consequently, the transmit signal at time positions k and $k + D_{\mathrm{s}}$ is identical for $k \in \{-D_{\mathrm{g}}, \ldots, D_{\mathrm{s}} - 1\}$. As long as the duration of the channel impulse response is shorter than the guard interval, this periodicity is preserved in the channel–distorted received signal and exactly this property is exploited for frame- and frequency synchronization purposes in [2].

For the analytical derivation and the simulation setup we assume the worst–case scenario that the — random–information carrying and therefore non–deterministic — preamble is embedded in a continuous sequence of random regular OFDM symbols. We assume equal average power for data and preamble symbols.

The transmitted (zero–mean) channel symbols (samples) obtained from the IDFT plus guard interval extension are denoted as s_k. Their average power is $\sigma_s^2 \stackrel{\mathrm{def}}{=} \mathcal{E}\{|s_k|^2\} = E_s/T$, where E_s is the average energy per channel symbol. In general, these T–spaced samples are convolved with the channel impulse re-

sponse and this yields some noiseless received signal $\tilde{r}_{0k}$. But here, we will restrict our investigation to a non–dispersive channel so that we have $\tilde{r}_{0k} = s_k$. The carrier frequency mismatch between transmitter and receiver oscillator is modelled in the baseband by rotating $\tilde{r}_{0k}$ with the absolute carrier frequency offset Δf_{co}. This yields the noiseless received sample $\tilde{r}_k = \tilde{r}_{0k}\mathrm{e}^{+\mathrm{j}2\pi\Delta f_{\mathrm{co}}kT} = \tilde{r}_{0k}\mathrm{e}^{+\mathrm{j}2\pi\xi_f\frac{k}{D}}$, where we introduced the normalized frequency offset (NFO) $\xi_f \stackrel{\mathrm{def}}{=} \frac{\Delta f_{\mathrm{co}}}{\Delta f_{\mathrm{sub}}}$. Note that the NFO is normalized to the subcarrier spacing of the regular OFDM symbols with D subcarriers as the demodulation performance of these data symbols is of interest. Non–perfect synchronization causes subcarrier interference [11], which spoils the transmission quality. Furthermore, insufficiently compensated NFOs cause a phase rotation between subsequent symbols. Clearly, the sensitivity of the transmission strongly depends on the type of data encoding and modulation. With lower–order differential modulation the NFO accuracy can be relaxed, while it gets increasingly stringent for large signal constellations. An important point is that due to normalization the performance degradation depends on the NFO only; the actual number of carriers D then has a marginal influence on the loss.

We assume zero–mean additive white Gaussian noise and therefore the received sample is $r_k = \tilde{r}_k + n_k$. The noise variance is $\sigma_n^2 \stackrel{\mathrm{def}}{=} \mathcal{E}\{|n_k|^2\} = N_0/T$, where N_0 is the power spectral density of white noise. Due to the non–dispersive channel we have $\mathcal{E}\{|\tilde{r}_k|^2\} = \sigma_s^2$ and the signal–to–noise power ratio (SNR) at the receiver input is $E_s/N_0 = \sigma_s^2/\sigma_n^2$.

3. Burst Synchronization

3.1. Frame Sync. Criteria and Frequency Estimation

An asymptotically optimum [8] frame synchronization metric in white Gaussian noise is the modified periodicity metric [2]

$$M_k \stackrel{\mathrm{def}}{=} \sum_{\kappa=0}^{D_\mathrm{s}-1} |r_{k+D_\mathrm{s}+\kappa}|^2 + \sum_{\kappa=0}^{D_\mathrm{s}-1} |r_{k+\kappa}|^2 - 2\,|S_k|\,,$$

where we introduced the complex correlation

$$S_k \stackrel{\mathrm{def}}{=} \sum_{\kappa=0}^{D_\mathrm{s}-1} r_{k+\kappa}^* r_{k+D_\mathrm{s}+\kappa}. \tag{1}$$

The estimation of the frame position is performed via

$$\widehat{k} = \underset{\tilde{k}}{\mathrm{argmin}}\; M_{\tilde{k}}, \tag{2}$$

which is a minimum search over various frame start hypotheses $\tilde{k}$. In the noiseless case M_k will be exactly zero for the ideal frame position(s). For finite SNRs in a non–dispersive channel the mean value of M_k will exhibit a constant–valued minimum within the guard interval region $-D_\mathrm{g} \le k \le 0$ (cf. Fig. 1c) so that a valid frame start will result.

A slightly different, optimum metric is proposed in [15]. Sometimes, the suboptimum frame synchronization metric [3]

$$\widehat{k} = \underset{\tilde{k}}{\mathrm{argmax}}\; |S_{\tilde{k}}| = \underset{\tilde{k}}{\mathrm{argmax}}\; |S_{\tilde{k}}|^2 \tag{3}$$

is proposed. In a non–dispersive channel, the magnitude of $\mathcal{E}\{S_k\}$ will exhibit a flat maximum in the guard interval (cf. Fig. 1b).

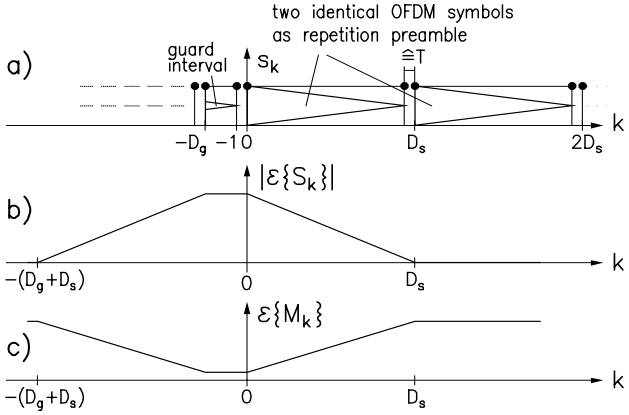

Figure 1: Symbolical illustration of the repetition preamble together with the expected values ($\mathcal{E}\{\cdot\}$) of the frame synchronization metrics M_k and S_k.

We mention that at SNRs larger than 1 the latter criterion is inferior to Eq. (2) in terms of false–lock probability [8].

Finally, we obtain the NFO estimate by evaluating S_k at the estimated frame start [2] and this yields

$$\widehat{\xi_f} = \frac{D}{2\pi D_\mathrm{s}} \arg\left(S_{\widehat{k}}\right).$$

Clearly, $|\xi_f| < D/(2D_\mathrm{s})$ is a minimum requirement to avoid ambiguity of this estimate, i.e., a reduction of D_s results in a larger lock–in range.

3.2. Frame Synchronization Performance

As depicted in Figs. 1c (1b), the mean value of M_k (S_k) exhibits a flat minimum (maximum) in a non–dispersive channel. Consequently, we expected a uniformly distributed lock–in probability in this region. For the simulation setup we will use $D = D_\mathrm{s} = 64$ with 53 active (non–zero) subcarriers and a guard interval of $D_\mathrm{g} = 8$. For completeness we mention the type of modulation in the subcarriers, although it has negligible impact on the time–domain behaviour and therefore does not affect any one of the results given in this paper. We used 4DPSK in the synchronization symbol and 8DPSK in the regular OFDM symbols. Simulation results of lock–in probabilities for the frame synchronization criteria in Eqs. (2) and (3) over a non–dispersive channel are given in Fig. 2 and we point out two observations.

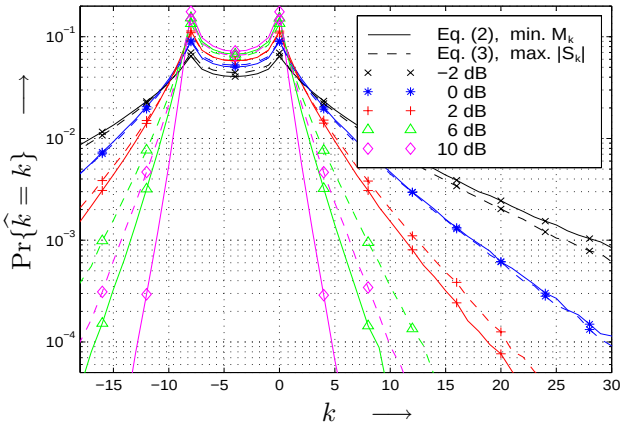

Figure 2: Simulated lock–in histogram in a non–dispersive channel at various $10\log_{10}(E_s/N_0)$ [dB]. The frame sync. criteria in Eqs. (2) and (3) are compared. The parameters are $D_\mathrm{s} = D = 64$ and $D_\mathrm{g} = 8$.

1.) At high SNRs criterion (2) shows a distinctly superior lock–in performance over criterion (3). The reason for this is the severely non–constant envelope of the OFDM signal [7], for which only (2) is accounting for. At SNRs lower than 1, (3) would be preferable.

2.) We find a surprising result in the guard interval region as the lock–in probabilities are quite perfectly symmetrical but non–uniformly distributed so that a hollow is formed in the middle.

The probability depression is unavoidable and turned out to be inherently systematic [10], giving motivation enough to further illuminate this result.

Hence, we want to introduce and calculate the probability $P_{k,g}$ that some time position k is estimated as frame start under the condition that it lies within some interval $[-g, 0]$ with $g \le D_\mathrm{g}$. In the end we have to set $g = D_\mathrm{g}$ to obtain the lock–in probability distribution of interest for a system with a guard interval of length D_g. In mathematical terms this conditional lock–in probability is

$$\begin{aligned} P_{k,g} &\overset{\text{def}}{=} \Pr\left\{M_k = \min \,\middle|\, k \in \{-g, \ldots, 0\}\right\} \\ &\approx \Pr\left\{|S_k| = \max \,\middle|\, k \in \{-g, \ldots, 0\}\right\} \\ &= \Pr\Bigg\{ \bigwedge_{\substack{\kappa=-g \\ \kappa\neq k}}^{0} \left(|S_k| > |S_\kappa|\right) \Bigg\}. \end{aligned}$$

We first assume that $P_{k,g}$ is somehow known and we would like to calculate

$$\begin{aligned} P_{k,g+1} &= \Pr\Bigg\{ \bigwedge_{\substack{\kappa=-(g+1) \\ \kappa\neq k}}^{0} \left(|S_k| > |S_\kappa|\right) \Bigg\} \\ &= \Pr\Bigg\{ |S_k| > \left|S_{-(g+1)}\right| \,\Bigg|\, \bigwedge_{\substack{\kappa=-g \\ \kappa\neq k}}^{0} \left(|S_k| > |S_\kappa|\right) \Bigg\} \\ &\quad \cdot \Pr\Bigg\{ \bigwedge_{\substack{\kappa=-g \\ \kappa\neq k}}^{0} \left(|S_k| > |S_\kappa|\right) \Bigg\} \overset{\text{def}}{=} t_{k,g} \cdot P_{k,g}\,, \end{aligned} \tag{4}$$

where we introduced the two–parametrical conditional probability $t_{k,g}$ with obvious definition. If we manage to calculate all required $t_{k,g}$, we can provide a recursive method to compute the conditional lock–in probabilities $P_{k,g}$ for any g, starting from the obvious $P_{k,0} = \Pr\left\{M_k = \min \,\middle|\, k \in \{0\}\right\} = \delta_{0k}$, where δ_{xy} is the Kronecker symbol. Hence, we obtain $P_{0,0} = 1$.

To take a first step in replacing the correlation magnitude $|S_k|$ with the received samples (cf. Eq. (1)), we introduce

$$w_k = r^*_{k+D_\mathrm{s}} r_{k+D_\mathrm{s}+D_\mathrm{s}} - r^*_k r_{k+D_\mathrm{s}}, \tag{5}$$

which can be interpreted as a differential correlation product.

With (1) and (5), we can easily confirm the two correlation recursions, respectively:

$$S_{k+n} = S_k + \sum_{\nu=k}^{k+n-1} w_\nu \quad ; \quad n \ge 0 \tag{6}$$

$$S_{k-n} = S_k - \sum_{\nu=k-n}^{k-1} w_\nu \quad ; \quad n \ge 0 \tag{7}$$

Note that due to the uncorrelatedness of the r_k — caused by random preamble, non–dispersive channel, and white noise —, the w_k themselves, represent a sequence of statistically independent zero–mean random variables as long as the observed interval is shorter than D_s. Hence, the w_ν which occur in the summations in (6) and (7) are statistically independent as long as $n < D_\mathrm{s}$. This is the case in practical systems, as usually $n \le D_\mathrm{g} < D_\mathrm{s}$.

We now observe the event $|S_k| > \left|S_{-(g+1)}\right|$ in (4) and with (7) we can provide an equivalent expression as

$$|S_k| > \left|S_{-(g+1)}\right| \;\Leftrightarrow\; |S_k| > \left|S_k - \sum_{\nu=-(g+1)}^{k-1} w_\nu\right|. \tag{8}$$

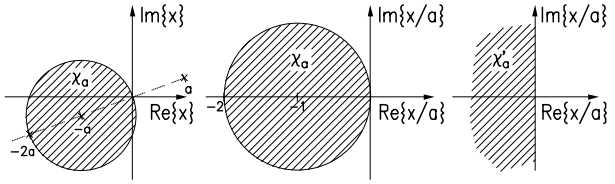

Figure 3: Exact set $\mathcal{X}_a$ and "approximate" set $\mathcal{X}'_a$ of complex numbers.

To further clarify this event, we take a look at the following set of numbers (with some $a \in \mathbb{C}\backslash\{0\}$)

$$\mathcal{X}_a = \left\{x \in \mathbb{C} \,\middle|\, |a + x| < |a|\right\} = \left\{x \,\middle|\, |1 + x/a| < 1\right\}. \tag{9}$$

This set is depicted in Fig. 3. For complex–valued random variables x with a probability density function (pdf) that is nearly zero for $|x| \ll |a|$, $\mathcal{X}_a$ can be replaced by (cf. Fig. 3)

$$\mathcal{X}'_a = \left\{x \in \mathbb{C} \,\middle|\, \Re\{x/a\} < 0\right\} \tag{10}$$

to compute the probability for — or to characterize — the set $\mathcal{X}_a$ approximately. The same idea is justified to simplify (8), as $|S_k| \gg \left|\sum_{\nu=-(g+1)}^{k-1} w_\nu\right|$ will be true. This is due to S_k having a large magnitude in the proximity of the correct synchronization point. The summation over a rather small number of w_ν will yield a significantly smaller magnitude.
Exploiting the above approximation we replace (8) by the approximate correspondence (indicated by $\overset{\approx}{\Leftrightarrow}$)

$$|S_k| > \left|S_{-(g+1)}\right| \;\overset{\approx}{\Leftrightarrow}\; \Re\Big\{\frac{1}{S_k}\sum_{\nu=-(g+1)}^{k-1} w_\nu\Big\} > 0 \quad (11)$$

to calculate $t_{k,g}$ in (4).
In (4) the probability for the event (11) is conditioned on the events $|S_k| > |S_\kappa|$ for $\kappa \in [-g,\, k-1]$ and for $\kappa \in [k+1,\, 0]$. With similar reasoning as above the approximate event relation

$$\begin{aligned} |S_k| > |S_\kappa| \;&\Leftrightarrow\; |S_k| > \Big|S_k + \sum_{\nu=k}^{\kappa-1} w_\nu\Big| \\ &\overset{\approx}{\Leftrightarrow}\; \Re\Big\{\frac{1}{S_k}\sum_{\nu=k}^{\kappa-1} w_\nu\Big\} < 0 \;;\; \kappa \in [k+1,\, 0] \quad (12) \end{aligned}$$

can be derived for the latter interval. Note that in (4) the conditioning on any one of the events in (12) does not affect the probability for the event $|S_k| > \left|S_{-(g+1)}\right|$, as the w_k's in the summation in (8) or (11) are disjoint to the ones in (12).
Exploiting this statistical independence of events, we can simplify $t_{k,g}$ and obtain

$$\begin{aligned} t_{k,g} &= \Pr\Big\{|S_k| > \left|S_{-(g+1)}\right| \;\Big|\; \bigwedge_{\substack{\kappa=-g \\ \kappa\neq k}}^{0} (|S_k| > |S_\kappa|)\Big\} \\ &= \Pr\Big\{|S_k| > \left|S_{-(g+1)}\right| \;\Big|\; \bigwedge_{\kappa=-g}^{k-1} (|S_k| > |S_\kappa|)\Big\}. \quad (13) \end{aligned}$$

The remaining conditioning events in (13) and their respective approximations are

$$\begin{aligned} |S_k| > |S_\kappa| \;&\Leftrightarrow\; |S_k| > \Big|S_k - \sum_{\nu=\kappa}^{k-1} w_\nu\Big| \\ &\overset{\approx}{\Leftrightarrow}\; \Re\Big\{\frac{1}{S_k}\sum_{\nu=\kappa}^{k-1} w_\nu\Big\} > 0 \;;\; \kappa \in [-g,\, k-1]. \quad (14) \end{aligned}$$

The division by S_k in (11) and (14) does not change anything, as the random variables w_ν are zero–mean and rotationally invariant in the limited region of interest. Thus, from (13) with (11) and (14), we finally obtain the approximation

$$\begin{aligned} t_{k,g} \;&=\; \Pr\Big\{ |S_k| > \left|S_{-(g+1)}\right| \;\Big|\; \bigwedge_{\kappa=-g}^{k-1} (|S_k| > |S_\kappa|) \Big\} \\ &\approx\; \Pr\Big\{ \Re\Big\{ \sum_{\nu=-(g+1)}^{k-1} w_\nu \Big\} > 0 \;\Big|\; \bigwedge_{\kappa=-g}^{k-1} \Big(\Re\Big\{ \sum_{\nu=\kappa}^{k-1} w_\nu \Big\} > 0 \Big) \Big\}. \quad (15) \end{aligned}$$

This is a probability, which only depends on the value of $u = k+g$, as $u+1$ represents the total number of elements in the summation of the event. The conditioning events have between 0 and u elements in the summation. Thus, the probability does not depend on the absolute values of k and g. Consequently, we state that $t_{k,g} = T_{k+g}$, where the newly introduced single–parameter value T_u is the u–th element ($u \in \mathbb{N}_0$) of some not yet known multiplicative factor sequence. For the 0–th multiplicative factor we obtain

$$T_0 = \Pr\{|S_{-g}| > |S_{-g-1}|\} \approx \Pr\{\Re\{w_{-g-1}\} > 0\} = \frac{1}{2},$$

as the w_ν are zero–mean random variables. The next element is

$$\begin{aligned} T_1 \;&=\; \Pr\Big\{|S_{-g+1}| > |S_{-g-1}| \;\Big|\; |S_{-g+1}| > |S_{-g}|\Big\} \\ &\approx\; \Pr\Big\{\Re\{w_{-g-1} + w_{-g}\} > 0 \;\Big|\; \Re\{w_{-g}\} > 0\Big\} > \frac{1}{2}. \end{aligned}$$

From (15) it becomes clear that asymptotically $T_u \to 1$ for $u \to \infty$ must be true. We interestingly found $T_u = \frac{2u+1}{2u+2}$ which still lacks a proof.

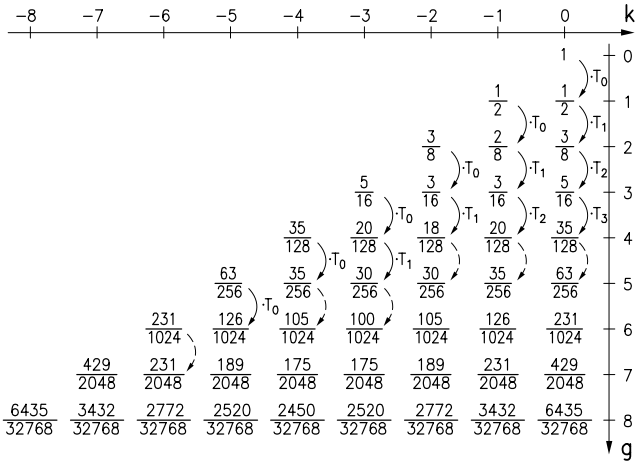

Table 1: Tabular calculation scheme for the conditional lock–in probabilities $P_{k,g}$ for $g \in \{0, \ldots, 8\}$ in non–dispersive channels.

The calculation scheme and a table of the conditional lock–in probabilities $P_{k,g}$ for guard intervals up to $D_g = 8$ is given in Tab. 1. The values for T_u can be determined easily in each recursion step from the symmetry property $P_{-k-g,g} = P_{k,g}$ and the probability distribution property $\sum_{k=-g}^{0} P_{k,g} = 1$. We give a short description of the process in calculating the row $g = 2$ from $g = 1$. With the known T_0 one can calculate the middle entry 2/8. From symmetry and the normalized sum, we obtain the two entries 3/8. Now we can determine $T_1 = 3/4$. The row $g = 3$ is derived from $g = 2$ via the known T_0 and T_1, which produces the middle entries (3/16). The outer entries (5/16) follow from

symmetry and that the probability sum must add to 1. Accordingly, $T_2 = 5/6$ follows.
To compare the analytically derived probabilities with the simulation results for a system with $D_\mathrm{g} = 8$, the conditional lock–in probabilities $P_{k,8}$ are plotted with circles in Fig. 4 and we see a perfect correspondence. We emphasize explicitly that the values of $P_{k,g}$ do neither depend on the variance nor on the exact pdf of the channel noise, so that already the smallest quantization noise will cause this depression effect for the lock–in probabilities.

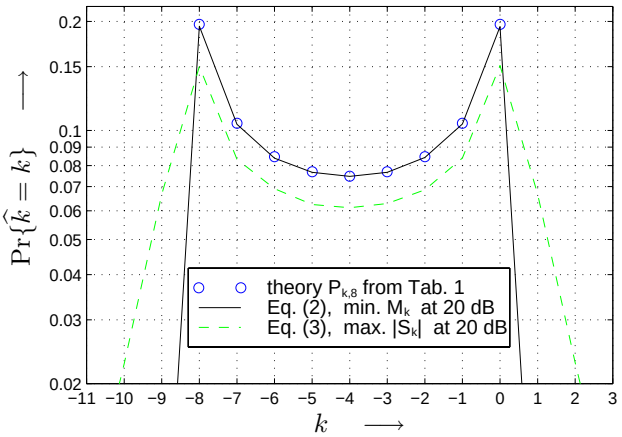

Figure 4: Simulated lock–in probabilities obtained with criteria in Eqs. (2) and (3) in a non–dispersive channel at $10\log_{10}(E_s/N_0) = 20$ dB. The theoretical results for the conditional lock–in probabilities $P_{k,8}$ are plotted for comparison (cf. Tab. 1).

The mismatch (shift) of the probabilities visible in Fig. 4 for criterion (3) is only due to severely frequent frame false–locks. Consequently, the sum of simulated lock–in probabilities in the guard region is significantly smaller than 1. If these probabilities were scaled appropriately (which means a parallel shift in the logarithmic scale), we again would achieve an almost perfect match of simulation and analytical prediction.
Let us summarize the main observation: Using random repetition preambles (Fig. 1a) over a non–dispersive channel leads to a system–inherent and noise–independent non–uniform lock–in probability distribution inside the guard interval. The outermost time positions are preferred over the middle ones. The desired perfect time position at $k = 0$ represents one of these two peaks, while the other one is $k = -D_\mathrm{g}$, which is mostly undesired. Consequently, depending on the specific application, some further frame sync. stage must be added to improve upon the coarse frame synchronization estimate.
In [12], no guard interval and only a deterministic preamble was considered so that the non–uniform distribution effect was not observed. Furthermore, a different frame synchronization metric was used.

3.3. Frequency Synchronization Performance

Being aware of the danger of slight frame synchronization failures, we are interested in the variance of the NFO estimate, when a frame synchronization error is present, i.e., the frame synchronization position does not lie within the guard interval region. In this case interfering signal portions from adjacent OFDM symbols are contained in $S_{\widehat{k}}$. Hence, we would like to calculate the variance of $\widehat{\xi_f}$ which is

$$\sigma^2_{\xi_f} = \frac{D^2}{4\pi^2 D_\mathrm{s}^2} \cdot \mathrm{var}\left(\arg\left(S_{\widehat{k}}\right)\right) \approx \frac{D^2}{4\pi^2 D_\mathrm{s}^2} \cdot \frac{\frac{1}{2}\sigma_S^2}{|\mu_S|^2} \quad (16)$$

with $\mu_S \overset{\mathrm{def}}{=} \mathcal{E}\{S_{\widehat{k}}\}$ and $\sigma_S^2 \overset{\mathrm{def}}{=} \mathrm{var}(S_{\widehat{k}})$. The approximation in (16) is due to an asymptotic result in [5], valid for $\sigma_S^2 \ll |\mu_S|^2$. It states that in this case $\arg(S_{\widehat{k}})$ is approximately Gaussian distributed with variance $\frac{1}{2}\sigma_S^2/|\mu_S|^2$. The required parameters can be approximated by (cf. Eq. (1)) $|\mu_S| \approx (D_\mathrm{s} - D_\mathrm{m})\,\sigma_s^2$ and by $\sigma_S^2 \approx 2D_\mathrm{s}\sigma_s^2\sigma_n^2 + D_\mathrm{s}\sigma_n^4 + D_\mathrm{m}\sigma_s^4$, where we introduced the frame misplacement $D_\mathrm{m} = f(\widehat{k}, D_\mathrm{g})$. D_m is an obvious function of the estimated frame position $\widehat{k}$ and the number of samples in the guard interval D_g. It counts the number of samples which represent intersymbol interference from adjacent OFDM symbols due to the non–optimum estimate $\widehat{k}$. For example if $D_\mathrm{g} = 8$ and $\widehat{k} = -10$, we would obtain $D_\mathrm{m} = 2$ and for $\widehat{k} = 1$ we would have to set $D_\mathrm{m} = 1$.
Incorporating the variance and mean into (16), we finally obtain

$$\sigma^2_{\xi_f} \approx \frac{D^2}{4\pi^2 D_\mathrm{s}^3} \cdot \frac{1}{(1 - D_\mathrm{m}/D_\mathrm{s})^2} \cdot \left(\frac{1}{E_s/N_0} + \frac{1}{2(E_s/N_0)^2} + \frac{D_\mathrm{m}/D_\mathrm{s}}{2}\right) \quad (17)$$

which represents a very good approximation for the variance of the NFO estimate, enabling two observations:
1) The frame misplacement causes an irreducible variance floor determined by the ratio $D_\mathrm{m}/D_\mathrm{s}$. The impact of this effect could be reduced by disregarding some outermost samples [14] in the correlation in (1).
2) The required preamble length for a prescribed normalized frequency accuracy rises only with $D_\mathrm{s} \sim D^{2/3}$ so that especially for very large D the preamble symbol size can be chosen considerably smaller.
In Fig. 5 we find simulation results for various fixed frame misplacements D_m and we see that for $D_\mathrm{m} \leq 8$, the simulation results at $\sigma_{\xi_f} = 10^{-2}$ are within 0.4 dB from (17).
The required standard deviation depends strongly on the specific modulation scheme in the subcarriers. For this, the subcarrier interference power as well as the residual phase rotation needs to be considered.
Due to channel–induced correlations in the received sample sequence, the effect of a moderate frame misplacement in dispersive channels is usually not as severe as in non–dispersive media. The estimation variance can easily fall short of Eq. (17). Hence, this analytical result is rather too pessimistic in dispersive

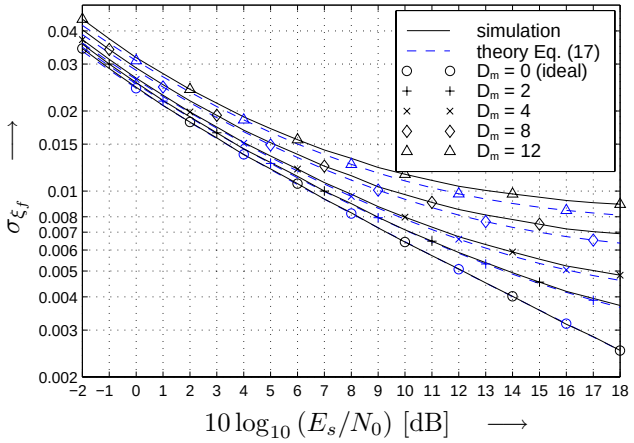

Figure 5: Simulation results and prediction from (17) for the NFO stdv σ_{ξ_f} over SNR with some fixed frame misplacement D_m as parameter.

channels, but we found it still in proximity of simulation results which are not given here.

4. Summary and Conclusions

We gave an analytical insight into a statistical effect which causes an amazing depression in the lock–in probability distribution of the frame synchronizer, when an OFDM repetition preamble according to [12], but now random and with guard interval is used in a non–dispersive channel. The effect can as well be observed in channels with moderate multipath echoes.

Furthermore, we provided a satisfying approximation for the variance of the NFO estimate for imperfect frame synchronization. This enables a robust design of the preamble length according to the specific system needs. Even though its derivation was performed for non–dispersive channels, the approximation in (17) may as well serve as a good approximation in dispersive channels.

By choosing preamble symbols with $D_\mathrm{s} \neq D$ a trade–off between accuracy, overhead and frequency lock–in range can be established.

The results in Fig. 5 allow the conclusion that the parameter choice used in the simulations for this paper enables a sufficiently accurate and robust frequency offset correction for the demodulation of 8DPSK or smaller signal constellations in time direction. Clearly, the frame synchronization performance depicted in Fig. 2 — especially at lower SNRs — is not satisfying for such short ($D = 64$) OFDM symbols. Too much interference is acquired by the rather frequent misalignments of the demodulation (DFT) window. An appropriate additional frame sync. stage must be implemented to allow an improved accuracy. One possibility to achieve more precision is the topic of current research to be published in near future.

References

[1] M. Alard and R. Lassalle. Principle of modulation and channel coding for digital broadcasting for mobile receivers. *EBU Review - Technical*, No.224:pp.168–190, 1987.

[2] P. R. Chevillat, D. Maiwald, and G. Ungerboeck. Rapid Training of a Voiceband Data–Modem Receiver Employing an Equalizer with Fractional–T Spaced Coefficients. *IEEE Trans. on Commun.*, vol.35,no.9:pp.869–876, 1987.

[3] T. Keller and L. Hanzo. Orthogonal Frequency Division Multiplex Synchronisation Techniques for Wireless Local Area Networks. In *Proceedings of the International Symposium on Personal, Indoor and Mobile Radio Communications (PIMRC'96)*, pages 963–967, Taipei, Taiwan, 1996.

[4] U. Lambrette, M. Speth, and H. Meyr. OFDM Burst Frequency Synchronization by Single Carrier Training Data. *IEEE Communications Letters*, vol.1,no.2:pp.46–48, 1997.

[5] B. C. Lovell and R. C. Williamson. The Statistical Performance of Some Instantaneous Frequency Estimators. *IEEE Transactions on Signal Processing*, vol.40,no.7:pp.1708–1723, 1992.

[6] P. H. Moose. A Technique for Orthogonal Frequency Division Multiplexing Frequency Offset Correction. *IEEE Trans. on Commun.*, vol.42,no.10:pp.2908–2914, 1994.

[7] S. Müller and J. Huber. A Comparison of Peak Power Reduction Schemes for OFDM. In *Proceedings of the Global Telecommunications Conference (GLOBECOM'97)*, pages 1–5, Phoenix, Arizona, USA, November 1997.

[8] S. Müller–Weinfurtner. *On the Optimality of Metrics for Coarse Frame Synchronization in OFDM: A Comparison.* To be presented at International Symposium on Personal, Indoor and Mobile Radio Communications (PIMRC'98). Boston, USA, September 1998.

[9] K. Pahlavan, A. Zahedi, and P. Krishnamurthy. Wideband Local Access: Wireless LAN and Wireless ATM. *IEEE Communications Magazine*, vol.35,no.11:pp.34–40, 1997.

[10] J. Rößler. *Analyse und Optimierung von Zeit- und Frequenzsynchronisationsalgorithmen für Mehrträgermodulationsverfahren.* Diplomarbeit am Lehrstuhl für Nachrichtentechnik, Universität Erlangen–Nürnberg (in German), August 1997.

[11] H. Sari, G. Karam, and I. Jeanclaude. Transmission Techniques for Digital Terrestrial TV Broadcasting. *IEEE Communications Magazine*, vol.33,no.2:pp.100–109, 1995.

[12] T. M. Schmidl and D. C. Cox. Robust Frequency and Timing Synchronization for OFDM. *IEEE Trans. on Commun.*, vol.45,no.12:pp.1613–1621, 1997.

[13] M. Speth, F. Classen, and H. Meyr. Frame synchronization of OFDM systems in frequency selective fading channels. In *Proceedings of the Vehicular Technology Conference (VTC'97)*, pages 1807–1811, Phoenix, Arizona, USA, 1997.

[14] B. Stantchev and G. Fettweis. Burst Synchronization for OFDM–based Cellular Systems with Separate Signaling Channel. In *Proc. of the Vehicular Technology Conference (VTC'98)*, Ottawa, Canada, May 1998.

[15] J.-J. van de Beek, M. Sandell, and P. O. Börjesson. ML Estimation of Time and Frequency Offset in OFDM Systems. *IEEE Transactions on Signal Processing*, vol.45,no.7:pp.1800–1805, 1997.